An improved theory for regenerative pump performance

T Meakhail and **S O Park**
Department of Aerospace Engineering, Korea Advanced Institute of Science and Technology, Taejon, Republic of Korea

The manuscript was received on 13 April 2004 and was accepted after revision for publication on 18 October 2004.

DOI: 10.1243/095765005X7565

Abstract: Owing to their low specific speed, regenerative pumps allow high heads with small flow rates and have performance curves with very stable features. This kind of pump is also smaller and simpler to construct than the other equivalent volumetric pumps, although it has fairly low efficiency. Over the past few years, regenerative pumps have been subject to more interest in various industrial applications. Previous mathematical models do not describe the flow characteristics very well as they are based on simplified assumptions. An improved model is proposed in this paper for the pump performance. The model can handle one inlet angle and two exit angles for the impeller blades and it can be used for the design of twisted blades that would increase the pump head and efficiency. A new feature of the pump characteristics based on the proposed model is discussed. It is shown that the proposed model yield results that are in good agreements with the experimental results. The new model also shows that the side-blade exit angle has a major effect on the performance of regenerative pump, which has not been accounted for in the previous theory.

Keywords: regenerative pump, circulatory flow, impeller angles, CFD

1 INTRODUCTION

Regenerative flow pumps and compressors have found many applications in industry; however they are the most neglected turbomachines in terms of research. The number of publications existing in the literature is comparatively less than papers dealing with centrifugal and axial turbomachines. Regenerative pumps are also known as peripheral pumps, side channel pumps, drag pumps, turbine pumps, traction pumps, tangential pumps, or vortex pumps. In contrast to other popular types of continuous flow machines in which the fluid passes through the impeller once, the regenerative machines have the fluid exposed to the impeller many times. The repetition of the action of the impeller blading on the fluid is, in effect, 'multi-staging', which makes regenerative machines capable of developing high-pressure ratios in a single impeller. Each passage through the vanes may be regarded as a conventional stage of compression. The main characteristic of a regenerative pump is its ability to generate high head at low flow rates. It has a very low specific speed and shares some of the characteristics of positive displacement machines such as root blowers, but without problems of lubrication and wear. In addition to self-priming characteristics, the main advantage offered by a regenerative pump is the ability to develop much higher heads than any other type of turbomachine with the same tip speed. When a regenerative flow pump/compressor (RFP and RFC) is applied as a gas compressor there is a further advantage of no surge or stall instability. Although the efficiency of RFP or RFC is not very high, usually less than 50 percent, they are used widely in industry. The RFP find applications in many industrial areas including automotive and aerospace fuel pumping, booster systems, water supply, agricultural industries, shipping and mining, chemical, and food processing systems. The RFC have been proposed for use in hydrogen gas pipelines and helium compressors for cryogenic applications in space vehicles [**1**].

Corresponding author: Department of Aerospace Engineering, Korea Advanced Institute of Science and Technology, 371-1 Kusong-dong, Yusong-gu, Taejon 305-701, Republic of Korea.

There are few mathematical models in literature, which explain the behavior of regenerative pumps and calculate their performance. Most of these models need extensive experimental support for performance prediction. Hence, it is very important from an industrial point of view to find efficient theoretical models that can be used to predict the regenerative pump performance in more details.

Wilson *et al.* [**2**] presented a simplified model to permit the development of a theoretical analysis of the three dimensional fluid motion inside a regenerative pump. He made several assumptions and applied fluid dynamic equations to arbitrary control volume of the pump. Iverson [**3**] analyzed regenerative pump performance in terms of shear stresses imparted to the fluid by the impeller. The performance equations were derived by considering a linear system with a linear motion of rough surface. A force balance on the fluid in the horizontal flow channel was applied to derive performance equations. Theories for the flow of compressible fluid in regenerative turbomachines are rarely found in the literature. Burton [**4**] made an effort in this direction and reported a simplified theory, which took account of area change and compressibility effects in regenerative turbomachines. The theoretical models discussed above used radial blade impellers. Sixsmith [**5**] replaced the radial blades by blades with an airfoil section and developed a theory. Song *et al.* [**1**] modified the momentum exchange theory by Wilson *et al.*[**2**] to the developing region of the regenerative pump. Their proposed model is effective for performance prediction at design point. However, owing to inaccuracy of some proposed loss models and slip factor correlations, it is not capable of accurately predicting the off-design flow conditions.

2 MOTIVATION

All the previous theories rely on assumptions not based on detailed measurements or detailed CFD calculations which would lead to better understanding of the complex flow inside the regenerative pump. For the configuration shown in Fig. 1, all the published work assumed that the outlet flow from the impeller blade occurs only at the tip of the impeller. Although Wilson *et al.* [**2**] mentioned that the previous experimental work showed that a part of the fluid leaves the impeller at the side of the blade, they assumed that all the flow leaves the impeller at the tip of the blades in their theoretical analysis. The CFD analysis carried out by the authors [**6**] showed that a part of the fluid leaves the impeller at the side of the blade as shown in Fig. 2. Figure 2(a) illustrates the velocity vectors at a middle cross

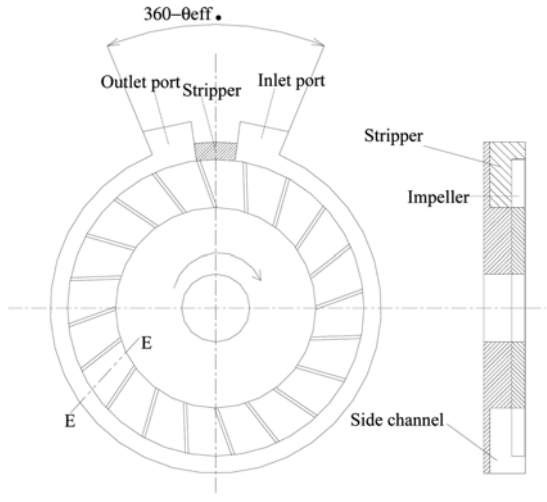

Fig. 1 Regenerative pump

section of the pump, section E–E of Fig. 1. Examining Fig. 2, we find that the flow enters the blade passage over nearly 60 percent of the blade height and leaves over about 40 percent of the blade height at its side, which illustrates the axial velocity component (or circulatory velocity V_m) at section G–G. The rest of the flow leaves at the blade tip as shown in Fig. 2(a).

As long as one part of the flow leaves the impeller at its tip and the other part leaves at its side, it becomes important to put the side angle and the tip angle as well as the inlet angle of the impeller in a mathematical model for performance prediction. This is graphically illustrated in Fig. 3 where we sketch helical flow paths for the previous theories

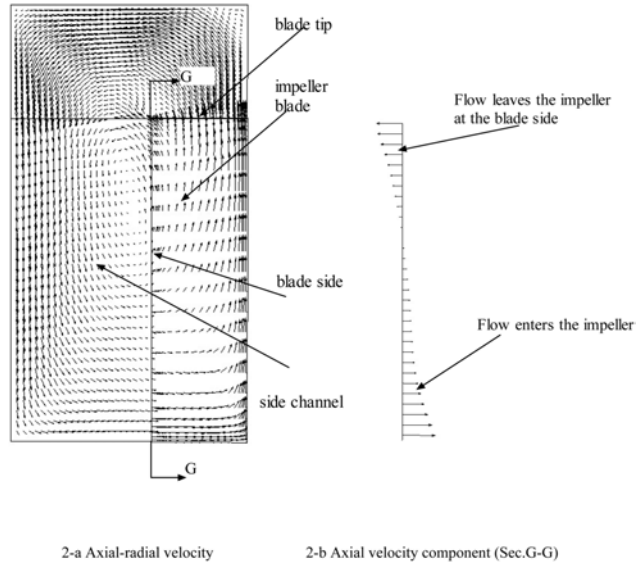

Fig. 2 Velocity vectors at section E–E: (a) axial–radial pump velocity; (b) axial velocity component (section G–G)

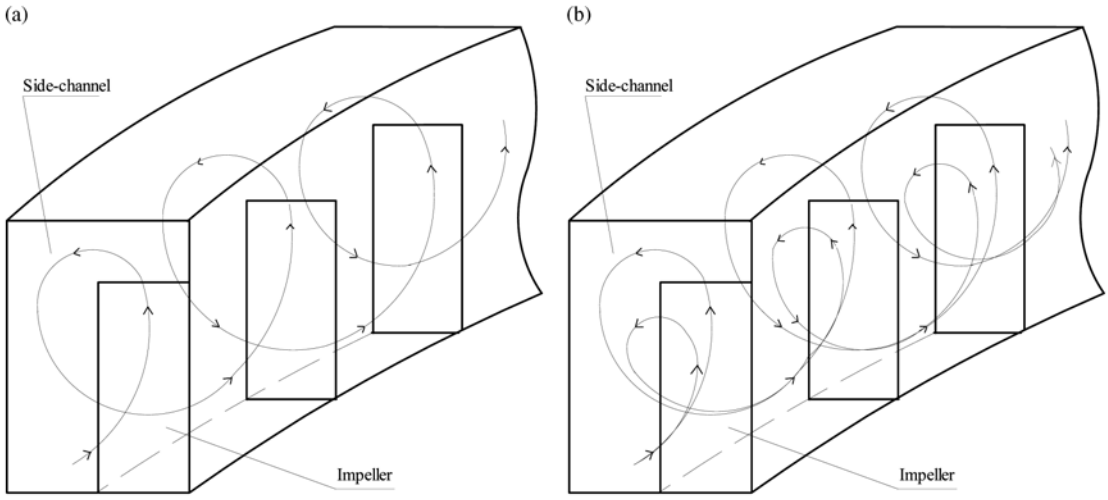

Fig. 3 Helical flow path. (a) Previous theory; (b) Present theory

and for the present theory. For more details of the flow mechanism and the velocity vectors around the blade, Fig. 4 shows the CFD results for two blades with different side angle (β_{2s}) at the blade tip and different inlet angle (β_1) for the same exit angle (β_{2t}; radial blades). From the figure, we find that the angles (β_1) and (β_{2s}) have a direct effect on the velocity vector around the blade at its

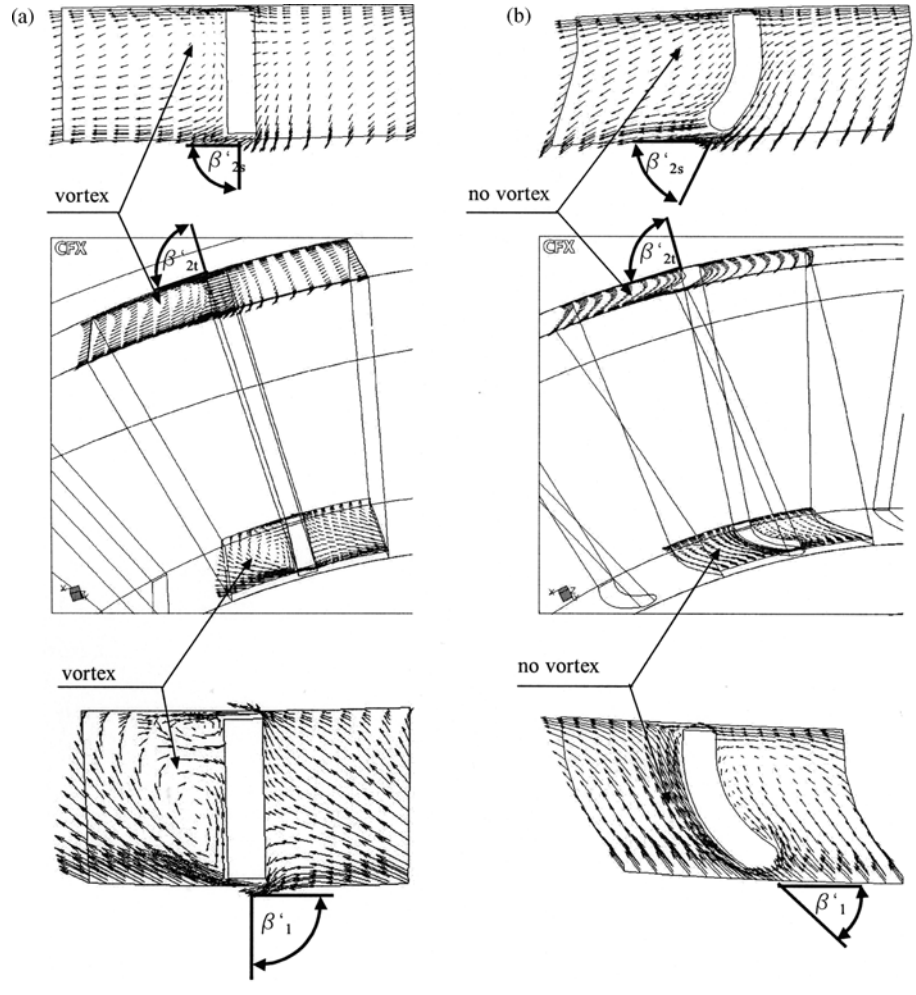

Fig. 4 Relative velocity vectors around the blade: (a) straight blade; (b) twisted blade

hub and its tip, which affect the performance of the pump.

Another important parameter that affects the performance is the number of circulations (n), which denotes the number of times of the flow passage through the impeller blades from the inlet port to the outlet port of the pump. The CFD results show that the flow enters the impeller at each blade passage. So, the number of circulations can easily be found as a function of the number of impeller blades (Z). Previous experiments done by Badami [**7**], showed that the number of impeller blades has a direct effect on the head developed by the pump.

From the discussions presented above, there appears to be a need for a new model, which involves the above parameters to describe the performance characteristics.

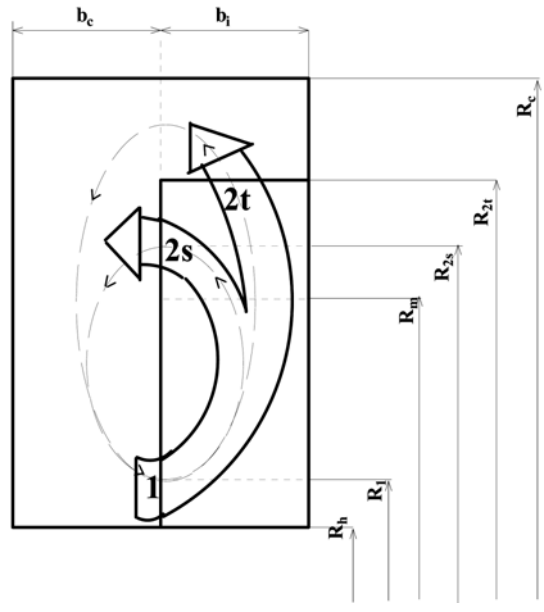

Fig. 5 Impeller and side channel dimensions

3 THE IMPROVED THEORY

The theory is based on the following assumptions and some CFD results:

(1) steady, incompressible flow;
(2) the helical flow can be described by the tangential velocity (V_u) and the circulatory velocity (V_m) along a mean streamline at any position;
(3) the flow enters the impeller at each blade passage; the number of circulations is equal to the number of the impeller blades excluding the part of stripper;
(4) part of the fluid leaves the impeller at its blade tip and another part leaves at its side (as discussed earlier);
(5) all irreversibilities can be categorized into the loss related to circulatory velocity or tangential velocity and are introduced as head losses.

For the mathematical formulation, we first specify the geometry of the impeller and side channel and draw the velocity triangles in Figs 5 and 6, respectively. Several radii in Fig. 5 are defined as

$$R_m = \sqrt{[0.5(R_{2t}^2 + R_h^2)}$$
$$R_1 = 0.5(R_m + R_h)$$
$$R_{2s} = 0.5(R_{2t} + R_m)$$

where R_h is hub radius and R_{2t} is the tip radius of the impeller.

3.1 Determination of the pump head

By applying the angular momentum equation per one circulation to the fluid in the side channel that is subjected to torque transmitted by the impeller, the expression for the head rise of the pump per one circulation, $h_{/cir}$, can be written as

$$gh_{/cir} = \frac{A_{2t}V_{m2t}R_{2t}V_{u2t} + A_{2s}V_{m2s}R_{2s}V_{u2s} - A_1V_{m1}R_1V_{u1}}{R_mA_c} \tag{1}$$

where Vs are the velocities depicted in Fig. 6 and As are the areas defined by

$$A_1 = \pi\left(\frac{R_m^2 - R_h^2}{Z}\right), \quad A_{2s} = \pi\left(\frac{R_{2t}^2 - R_m^2}{Z}\right),$$
$$A_{2t} = \frac{2\pi R_{2t}b_i}{Z}, \quad A_c = (R_c - R_h)b_c + (R_c - R_{2t})b_i$$

where Z is the number of impeller blades, b_i the impeller width, b_c the side channel width, and R_c the outer radius of the side channel.

Equation (1) is the same equation obtained by Wilson *et al.* [**2**] and Badami [**7**] except for the difference that it contains the term ($A_{2s}V_{m2s}R_{2s}V_{u2s}$), which represents the momentum of the fluid leaving at the side of the impeller blade. This term is a function of the side exit angle of the impeller since V_{u2s} is given by

$$V_{u2s} = (U_{2s} - V_{m2s}\cot\beta_{2s}) \tag{2}$$

Similarly, we have

$$V_{u2t} = (U_{2t} - V_{m2t}\cot\beta_{2t}) \tag{3}$$

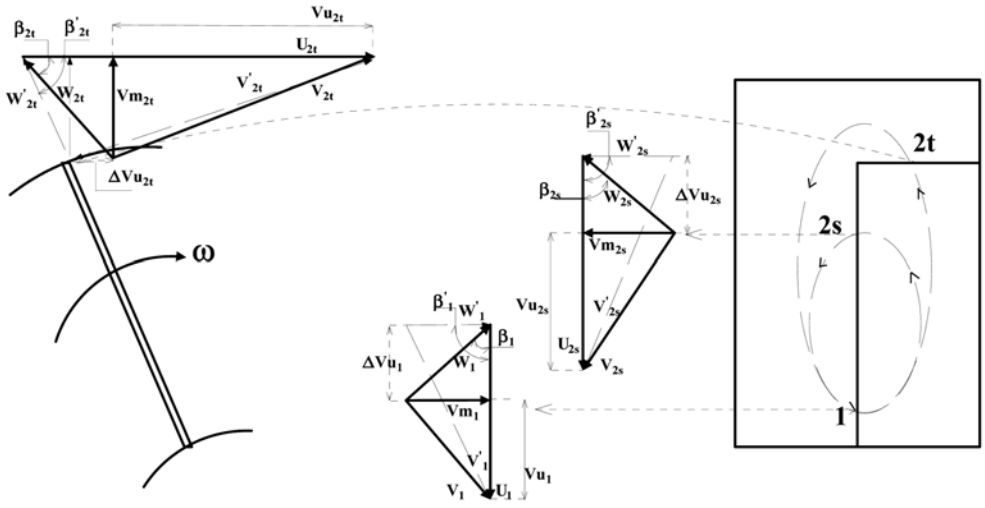

Fig. 6 Velocity triangle

where

$$U_{2t} = \omega R_{2t},\ U_{2s} = \omega R_{2s}, \text{ and } \omega = 2\pi N/60.$$

To render these velocities more realistic, slip factors need to be considered. The slip factor is introduced to account for the degree of flow guidance by the blade for outgoing flow at its tip (2t) and its side (2s) is defined as the ratio of the real tangential velocity to the ideal tangential velocity. Among several slip factor correlations, Grabow's [**8**] model was chosen. The slip correlation at the blade side is

$$\sigma_s = \frac{1}{\{1 + 2.5[1 + \sin(\beta'_{2s} + 90)]/Z\}} \tag{4}$$

Similarly, at the blade tip, we have

$$\sigma_t = \frac{1}{\{1 + 2.5[1 + \sin(\beta'_{2t} + 90)]/Z\}} \tag{5}$$

where β'_{2s} and β'_{2t} are the blade exit angles at the blade side and blade tip, respectively.

Then, equations (2) and (3) can be rewritten as

$$V_{u2s} = \sigma_s(U_{2s} - V_{m2s}\cot\beta'_{2s}) \quad \text{and}$$

$$V_{u2t} = \sigma_t(U_{2t} - V_{m2t}\cot\beta'_{2t})$$

The circulatory flow velocities, V_{m1}, V_{m2s}, and V_{m2t} can be calculated by using the theoretical consideration presented in Appendix 2.

The tangential velocity in the side channel, V_c, can be calculated as

$$V_c = \frac{Q}{A_c} \tag{6}$$

By assuming that V_c is the average of the tangential components V_{u1} and V_{u2t}, we have

$$V_{u1} = 2V_c - V_{u2t} \tag{7}$$

The total head of the pump can be expressed as

$$H = nh_{/cir} - \frac{1}{2g}K_p\left(\frac{Q}{A_c}\right)^2 \tag{8}$$

The head coefficient is given by

$$\psi = \frac{gH}{N^2D_{2t}^2} - K_p\phi^2 \tag{9}$$

where ϕ is the flow coefficient. K_p is the loss coefficient corresponding to the pressure drop in the inlet and outlet ports, which is to be found by equating the theoretical and experimental head coefficients as done in previous theories [**2**, **7**, **9**].

The number of circulation n can be simply calculated from

$$n = \frac{\theta_{eff}}{360}Z \tag{10}$$

where θ_{eff} is the effective angle of the pump from the inlet port to the outlet port as shown in Fig. 1.

3.2 The hydraulic efficiency and losses in the flow path

To determine the hydraulic efficiency, we need to evaluate the power input to the impeller P_i and the real flow rate Q_r since the hydraulic efficiency η_h is

given by

$$\eta_h = \frac{\rho Q_r g H}{P_i} \tag{11}$$

To evaluate the power input to the impeller, the losses inside the pump should be estimated. The losses inside the pump can be categorized as follows:

(1) Tangential head loss in the side channel h_c and it can be calculated as a function of the average tangential velocity in the side channel V_c by

$$gh_c = \frac{1}{2}\xi_c V_c^2 \tag{12}$$

where ξ_c is the channel skin friction loss given by applying the classic pipe-loss formula using the concept of hydraulic diameter D_h of the side channel and length of the side channel L [**10**].

$$\xi_c = \lambda_f \frac{D_h}{L}$$
$$\lambda_f = \lambda_o \left[1 + 0.075 Re^{0.25} \left(\frac{D_h}{2R_t}\right)^{0.5}\right]$$
$$\lambda_o = 0.316 Re^{-0.25}$$

(2) Direct loss in the impeller h_i and it includes losses due to friction, turning, contraction, and sudden expansion. It is proportional to the relative velocity in the impeller and is calculated by

$$gh_i = \frac{1}{2}\xi_i W_{2t}^2 \tag{13}$$

where the loss coefficient ξ_i is to be evaluated experimentally [**7**, **9**]. By summing the two losses above, the total friction power losses P_f can be calculated as

$$P_f = \rho g Q_c (h_i + h_c) \tag{14}$$

(3) Incidence loss h_{in} is assumed to be caused by the difference between the blade angle and the flow angle when the fluid enters the blade region and is estimated as the difference in tangential velocity ΔV_{u1}, which is given by

$$\Delta V_{u1} = (U_1 - V_{u1} - V_{m1} \cot \beta_1')$$

where β_1' is the inlet blade angle and $U_1 = \omega R_1$. The incidence loss is then estimated by

$$gh_{in} = \frac{1}{2}\Delta V_{u1}^2 \tag{15}$$

The incidence power loss P_{in} can be calculated as

$$P_{in} = \rho g Q_c h_{in} \tag{16}$$

3.3 Input power to the impeller

The input power to the impeller is equal to the output power plus the summation of losses inside the pump. Equation (8) can also be rewritten as

$$H = H_c - H_{ic} \tag{17}$$

where H_c is the total head imparted from the impeller to the fluid in the side channel and H_{ic} is the head loss in the inlet and outlet ports.

The total power imparted from the impeller P_c can be calculated as

$$P_c = \rho g Q H_c \tag{18}$$

The power input to the impeller P_i will be consumed in [**2**, **9**]:

(1) power required for pumping the fluid to the required pressure P_c;
(2) power required to overcome the friction loss in the impeller and side channel P_f;
(3) power required to overcome incidence loss at the inlet of the impeller blades P_{in}.

Thus, the total input power P_i is given by

$$P_i = P_c + P_f + P_{in} \tag{19}$$

3.4 Leakage flow rate

The real flow rate Q_r required by a pump is less than the flow rate Q through the pump because of existence of the leakage flow Q_l. The leakage flow rate can be calculated as

$$Q_l = C_d A_{cl} \sqrt{2gH} \tag{20}$$

where C_d indicates friction drag coefficient for leakage flow and can be calculated as [**11**]

$$C_d = \frac{1}{\sqrt{\lambda_f (L/D_h) + 1.5}}$$

and A_{cl} indicates the clearance area.

The real flow rate can be calculated as

$$Q_r = Q - Q_l \tag{21}$$

4 RESULTS AND DISCUSSION

4.1 Performance comparison

In order to estimate the proposed one-dimensional flow model, the results of the model were compared with the experimental data. The experiments done by Meakhail *et al.* [**12**], Abdou *et al.* [**9**], and Abd El-Messih *et al.* [**13**] for the same pump have been selected for the validation study of the new model. The pump was tested at 1200 rpm. The principal geometrical characteristics of the pump are:

- impeller diameter ($D_{2t} = 170$ mm);
- inlet blade angle ($\beta'_1 = 90^\circ$);
- outlet blade angle at its side ($\beta'_{2s} = 90^\circ$);
- outlet blade angle at its tip is ($\beta'_{2t} = 70^\circ$);
- number of blades ($Z = 20$).

Empirical values of ξ_i and K_p were determined such that the experimental and the theoretical head coefficients agreed with each other. It was found that $\xi_i = 0.65$ and $K_p = 0.01$ gave the best agreement, which means that the losses inside the impeller are much higher than those in the inlet and outlet ports.

Figure 7 shows the theoretical and experimental head coefficient vs flow coefficient. The agreement between the theoretical and experiment curves is good. The curve is nearly linear and its slope downward. This agrees very well with the well-known characteristics of regenerative pump. The theoretical and experimental head coefficients for another impeller with different angles ($\beta'_1 = 135^\circ$, $\beta'_{2s} = 135^\circ$, and $\beta'_{2t} = 90^\circ$) is also plotted in Fig. 8. It was found

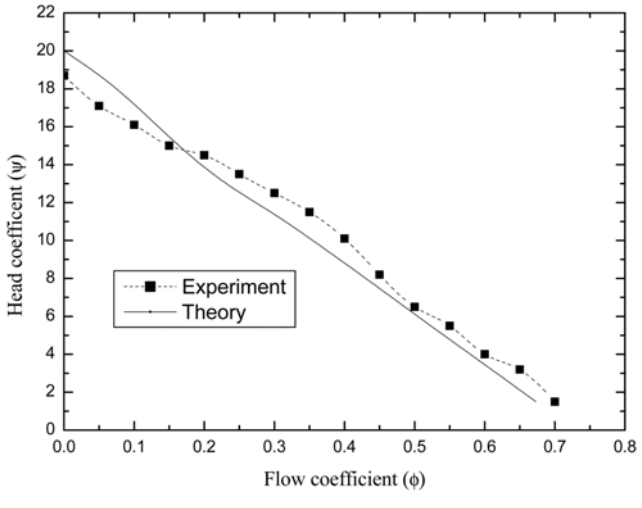

Fig. 7 Prediction vs experimental data head coefficient ($\beta'_1 = 90^\circ$, $\beta'_{2s} = 90^\circ$, and $\beta'_{2t} = 70^\circ$ [**9**])

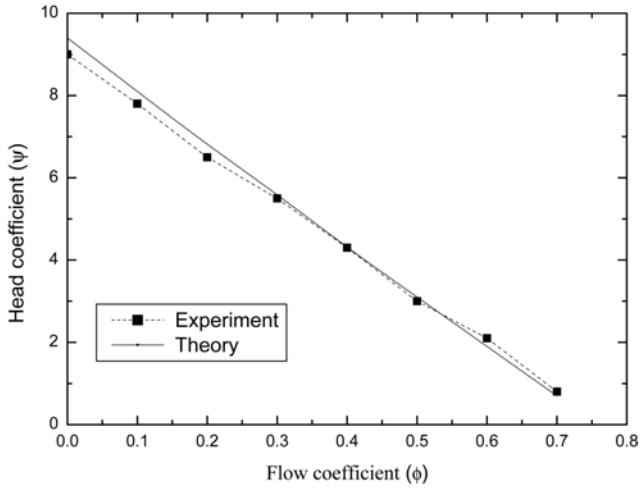

Fig. 8 Prediction vs experimental data head coefficient ($\beta'_1 = 135^\circ$, $\beta'_{2s} = 135^\circ$, and $\beta'_{2t} = 90^\circ$ [**13**])

that the same coefficients $\xi_i = 0.65$ and $K_p = 0.01$ give the best agreement. Further performance prediction is made for a different pump to assure the applicability of the present model [**2**, **14**]. The empirical coefficients of $\xi_i = 0.65$ and $K_p = 0.01$ were used in the calculation and the result is given in Fig. 9. The predicted and the experimental data are in good agreement.

It must be pointed out here that, the number of circulations is the same for the same impeller at different operating conditions since the fluid enters and circulates each impeller passage the same way as shown in Figs 2 and 4. The question raised would be: 'what mechanism is responsible for the known characteristics of regenerative pumps? or

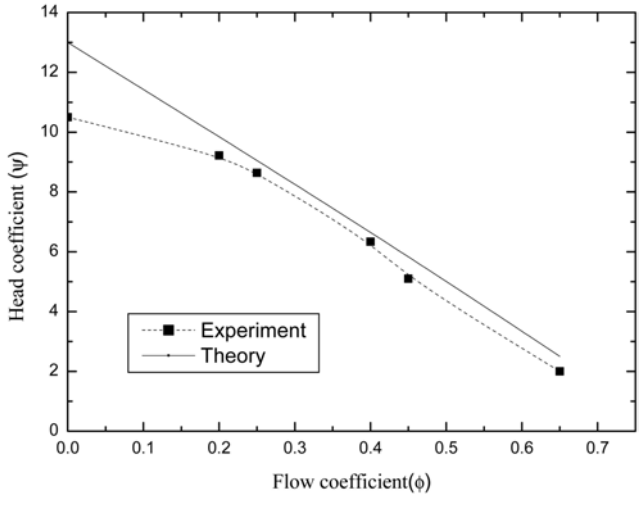

Fig. 9 Prediction vs experimental data head coefficient [**2**, **14**]

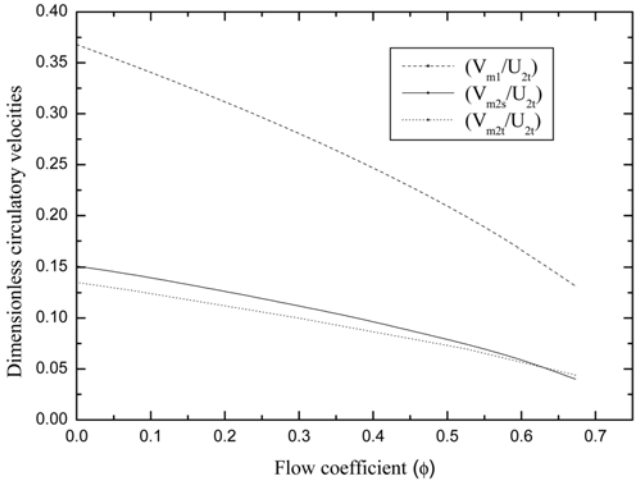

Fig. 10 Circulatory flow velocities

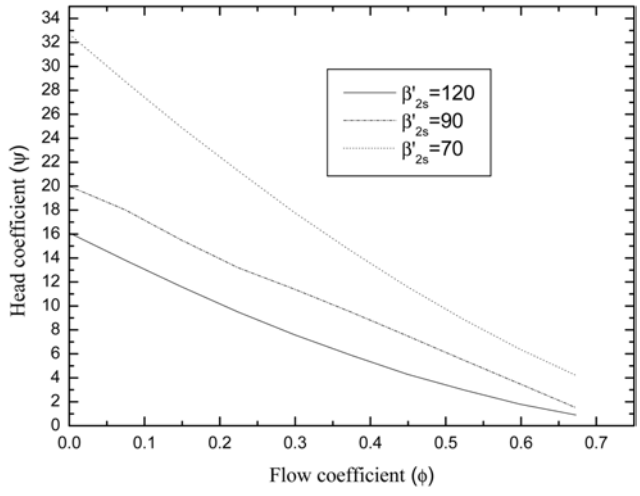

Fig. 11 Effect of side-blade exit angle on the head coefficient

what is the mechanism responsible for the sharp increase in head with decreasing the flow rate?'. Figure 10 explains the variation of dimensionless circulatory (meridional) flow velocities, V_{m1}/U_{2t}, V_{m2s}/U_{2t}, and V_{m2t}/U_{2t} [which can be calculated from equations (A6), (A4), and (A3), respectively] with the flow rate. Decreasing the flow rate will increase the circulatory flow velocity at the inlet of the impeller blade V_{m1} and increase the circulatory flow velocity at the blade tip V_{m2t} as well as at the blade side V_{m2s}. Equation (1) shows that increasing V_{m2t} and V_{m2s} will increase the head of the pump. Such a flow characteristic makes the regenerative pumps more useful for applications requiring high head at low flow rates.

4.2 Effect of side-blade exit angle (β'_{2s})

The contribution of the new theory is to show the effect of changing the side-blade exit angle (β'_{2s}) of the impeller on the performance of regenerative pump. Figure 11 shows this effect. It is clear that the exit angle (β'_{2s}) has a significant effect on the performance. At a point close to the best efficiency point ($\phi = 0.45$), the head coefficient increases by 55 per cent when the angle decreases from 90 to 70° and it decreases by 37 per cent when the angle increases from 90 to 120°. This effect was not accounted for in the old theory [**2**] as the old theory does not contain the term of the momentum of the fluid leaving at the side of the impeller blade ($A_{2s}V_{m2s}R_{2s}V_{u2s}$) expressed in equation 1. This effect is felt at lower flow coefficient as shown in Fig. 11. The influence of β'_{2s} on hydraulic efficiency is illustrated in Fig. 12. When the angle β'_{2s} decreases from 90 to 70°, the hydraulic efficiency increases from 45 per cent to about 55 per cent and decreases to about 30 per cent when $\beta'_{2s} = 120°$ near the best efficiency point. The main reason for the lower head and lower hydraulic efficiency for cases with $\beta'_{2s} = 90$ and 120° is the formation of vortex behind the blade because the flow angle in these cases is very different from the blade angle. For the case with β'_{2s} smaller than 90°, the flow angle is close to the blade angle and hence there is no vortex formation behind the blade leading to higher efficiency. These results agree qualitatively well with the CFD analysis depicted in Fig. 4.

5 CONCLUSIONS

In this work, an improved theory is proposed for the regenerative pump performance. The theory can

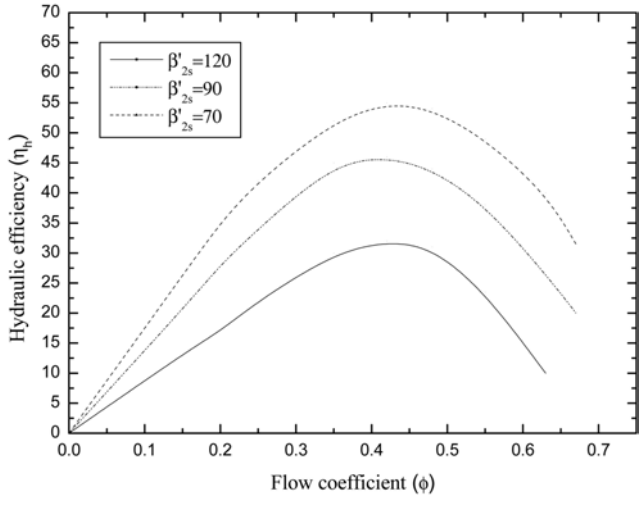

Fig. 12 Effect of side-blade exit angle on the hydraulic efficiency

handle one inlet angle and two outlet angles of the impeller blades as well as the number of circulations. By comparing the results from a one-dimensional performance model and those obtained from test, it was concluded that the proposed model is more suitable for performance prediction. The mechanism responsible for the sharp increase of pump head with decreasing flow rate is the increase of circulatory flow velocity with decreasing flow rate. The special feature of the new model is that it can account for the effect of side-blade exit angle, which has a major effect on the regenerative pump performance.

ACKNOWLEDGMENT

The authors are grateful to the Brain-Korea 21 at KAIST for supporting this work.

REFERENCES

1 **Song J. W., Engeda A.,** and **Chung M. K.** A modified theory for the flow mechanism in a regenerative flow pump. *Proc. Instn Mech. Engrs Part A: J. Power and Energy*, 2003, **217**, 311–321.
2 **Wilson, W. A., Santalo, M. A.,** and **Oelrich, J. A.** A theory of the fluid-dynamic mechanism of regenerative pumps. *Trans. ASME*, 1955, **77**, 1303–1316.
3 **Iverson, H. W.** Performance of the periphery pump. *Trans. ASME*, 1955, **77**, 19–28.
4 **Burton, D. W.** Review of regenerative compressor theory. *Rotat. Machin. Gas-Cooled Reactor Applic.*, 1962, **TID-7631**, 228–242.
5 **Sixsmith, H.** and **Altmann, H.** A regenerative compressor. *Trans. ASME J. Engng Ind.*, 1977, **99**, 637–647.
6 **Meakhail, T., Seung O. P., Dae Sung Lee,** and **Mikhail S.** A study of circulating flow in regenerative pump. Proceedings of the *KSAS 1st International Session*. 2003, Gyeongju, pp. 19–26.
7 **Badami, M.** Theoretical and experimental analysis of traditional and new periphery pumps. SAE Technical Paper Series, no. 971074, 1997, pp. 45–55.
8 **Grabow, G.** Influence of the number of vanes and vane angle on the suction behavior of regenerative pumps. Proceedings of *Second Conference on Flow Machines*, October 1966, Budapest, pp. 147–166.
9 **Abdou, H., El-sallak, M.,** and **Mikhail, S.** Effect of some geometrical variables on performance of peripheral pumps. M.Sc. Thesis, Faculty of Engineering, Cairo University, 1996.
10 **Fox, R.** and **McDonald, A.** *Introduction to Fluid Mechanics* 1998 (John Wiley and Sons, New York).
11 **Stepanoff, A. J.** *Centrifugal and Axial Flow Pumps*, 1957 (John Wiley & Sons, New York).
12 **Meakhail, T., El-sallak, M., Serag-Eldin, M. A.,** and **Mikhail, S.** Effect of guide blades fixed in the side channel on performance of peripheral pumps. M.Sc. Thesis, Faculty of Engineering, Cairo University, 1996.
13 **Abd El-Messih, R.** and **Mikhail, S**. Investigation of some design elements on the performance of peripheral pumps. M.Sc. Thesis, Faculty of Engineering, Cairo University, 1975.
14 **Senoo, Y.** A comparison of regenerative pump theories supported by new performance data. *Trans. ASME*, 1956, **78**, 1091–1102.

APPENDIX 1

Notation

A	cross sectional area
b	width of the impeller or channel
h	head loss
H	head
n	number of circulations (number of times the fluid passes through the impeller blades)
N	rotational speed (rpm)
p	pressure
P	power
Q	flow rate
r	radius
U	peripheral velocity
V	absolute velocity
W	relative velocity
Z	number of impeller blades
β'	blade angle (the theoretical angle of the flow)
β	flow angle (the actual angle of the flow)
ρ	density
σ	slip factor
θ_{eff}	effective angle from the inlet to the outlet of the pump
ω	rotational speed
ϕ	flow coefficient ($Q/A_c R_m \omega$)
ψ	head coefficient (gH/N^2D^2)

Subscripts

1	position of inlet flow to the impeller blade
2s	position of outlet flow from the impeller side
2t	position of outlet flow from the impeller tip
c	channel
cir	circulation
h	hub
i	impeller
in	incidence
m	meridional (circulatory)component, mean value
s	side
t	tip
u	tangential component

APPENDIX 2

Circulatory flow velocity calculations

The unknown parameters in equations (1)–(3) are the circulatory or merdional flow velocities (V_{m1}, V_{m2s} and V_{m2t}) and can be calculated as follows.

Applying the energy equation to the blade region between points (1) and (2t) shown in Fig. 5, we obtain

$$\frac{p_1}{\rho}+\frac{1}{2}V_1^2+(U_{2t}V_{u2t}-U_1V_{u1}) = \frac{p_{2t}}{\rho}+\frac{1}{2}V_{2t}^2+gh_{1-2t} \tag{A1}$$

where

$$gh_{1-2t}=\frac{1}{2}\xi_i W_{2t}^2$$

and to the channel region:

$$\frac{p_{2t}}{\rho}+\frac{1}{2}V_{m2t}^2+\frac{1}{2}V_{c2t}^2=\frac{p_1}{\rho}+\frac{1}{2}V_1^2+gh_{2t-1} \tag{A2}$$

where

$$gh_{2t-1}=\frac{1}{2}\xi_c V_c^2$$

By summing equations (A1) and (A2) and substituting the above values, a second-order equation for circulatory velocity at the blade inlet, V_{m2t}, is obtained as

$$\frac{\xi_i}{2\sin^2\beta_{2t}}(V_{m2t}^2)+\sigma_t(U_{2t}+U_1)\cot\beta_{2t}(V_{m2t}) + \frac{\xi_c}{2}\left(\frac{Q}{A_c}\right)^2+2\frac{U_1Q}{A_c}-\sigma_t(U_{2t}+U_1)U_{2t}=0 \tag{A3}$$

Similarly, applying the energy equation to the blade region between points (1) and (2s), and to the channel region, an expression for V_{m2s} is also obtained.

$$\frac{\xi_i}{2\sin^2\beta_{2s}}(V_{m2s}^2)+\sigma_s(U_{2s})\cot\beta_{2s}(V_{m2t}) + \frac{\xi_c}{2}\left(\frac{Q}{A_c}\right)^2+U_1(2V_c-V_{u2t})-\sigma_s U_{2s}^2=0 \tag{A4}$$

From the continuity equation, we have

$$A_1V_{m1}=A_{2t}V_{m2t}+A_{2s}V_{m2s} \tag{A5}$$

Thus,

$$V_{m1}=\frac{A_tV_{m2t}+A_{2s}V_{m2s}}{A_1} \tag{A6}$$